1-1-2012

Stability Analysis of an Autonomous Microgrid Operation Based on Particle Swarm Optimization

Waleed Al-Saedi

Stefan Lachowicz
Edith Cowan University

Daryoush Habibi
Edith Cowan University

Octavian Bass
Edith Cowan University

10.1109/PowerCon.2012.6401291

Stability Analysis of an Autonomous Microgrid Operation Based on Particle Swarm Optimization

Waleed Al-Saedi, *Student Member*, *IEEE*, Stefan W. Lachowicz, *Senior Member*, *IEEE*, Daryoush Habibi, *Senior Member*, *IEEE*, and Octavian Bass, *Senior Member*, *IEEE*

***Abstract*—This paper presents the stability analysis for an inverter based Distributed Generation (DG) unit in an autonomous microgrid operation. The small-signal model of the controlled Voltage Source Inverter (VSI) system is developed in order to investigate the dynamic stability for the given operating point and under the proposed power controller. This model includes all the details of the proposed controller, while no switching actions are considered. System oscillatory modes and the sensitivity to the control parameters are the main performance indices which are considered, particularly when the microgrid is islanded or under the load change condition. In this work, the proposed power controller is composed of an inner current control loop and an outer power control loop, both based on a synchronous reference frame and conventional PI regulators. These controllers also utilize the Particle Swarm Optimization (PSO) for real-time self-tuning in order to improve the quality of the power supply. The complete small-signal model is linearized and used to define the system state matrix which is employed for eigenvalue analysis. The results prove that the stability analysis is fairly accurate and the controller offers reliable system's operation.**

***Index Terms*—Microgrid, power controller, Particle Swarm Optimization (PSO), small-signal stability.**

I. Introduction

A MICROGRID is a recent innovation of the small-scale power generation network that aggregates a cluster of DG units using power electronic devices such as the VSI system. This scenario can represent a complementary infrastructure to the utility grid due to the rapid change of the load demand. The high market penetration of the micro-sources such as wind, photovoltaic, hydro, and fuel cell emerge as alternatives which provide green energy and a flexible extension to the utility grid [1]. These sources are usually connected to the power system by widely used Pulse-Width-Modulation (PWM)-VSI systems. While they offer flexible control and operation compared to the conventional power generators, the microgrid is more susceptible to the oscillations occurring across the system due to network disturbances such as fault or load change [2].

An example of the microgrid is shown in Fig. 1, grid-connected and islanding being the two operation modes of this system [1]. In grid-connected mode, the grid dominates most of the system dynamics and no significant issues need to be addressed except the power flow control, whereas in the islanding mode, once the isolating switch disconnects the utility due to network fault or market decision, the micro-sources directly influence the system dynamics, thus a reliable operation can be only achieved by adopting an adequate control mode.

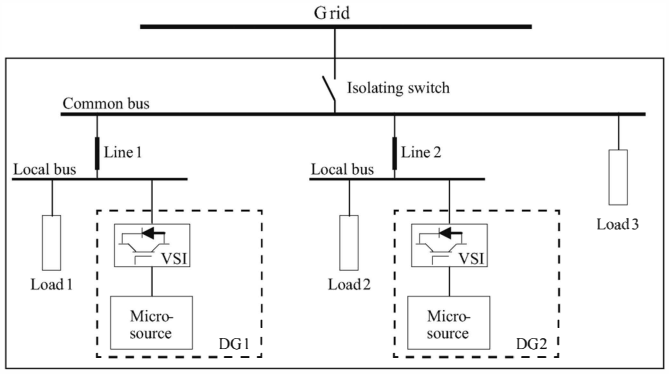

Fig. 1. An example of the microgrid

The small-signal stability is one of the most important issues of the system's reliable operation. It can be defined as the ability of the power system to return to normal operating condition following a small physical disturbance. The stability analysis substantially depends on the linearized state-space equations that define the characteristics of the power system model. Thus, stability can be easily studied by determining the solution of the system characteristic equation [3].

The problem of dynamic stability of the microgrid is being increasingly important and directly influenced by the network dynamics, a well-established model of the inverter and its control loops is necessary to obtain realistic evaluation of the system's operation [4]. For the stand-alone mode, the small-signal state-space analysis of the microgrid is well developed in [5], the system is modeled to identify the oscillatory modes for the transient response, and the sensitivity analysis is also considered which aims at evaluating the designed controller. In [6], the small-signal model is presented to assess the proposed power management strategies, and also to find the optimum values of the control parameters.

In this paper, the small-signal state-space model is developed for an individual inverter based DG unit in autonomous microgrid operation. An optimal power controller is proposed for voltage and frequency regulation. This controller is composed of an inner current control loop and an outer power control loop. The PSO algorithm is an intelligent search process that is incorporated to find the optimal power control parameters when the microgrid transits to the islanding mode

The authors are with the School of Engineering, Faculty of Computing, Health and Science, Edith Cowan University, Perth, Western Australia (e-mail: walsaedi@our.ecu.edu.au, s.lachowicz@ecu.edu.au, d.habibi@ecu.edu.au, and o.bass@ecu.edu.au).

978-1-4673-2868-5/12/$31.00 ©2012 IEEE

or during the load change condition. In this work, the small-signal dynamic model is constructed for the given operating point in order to investigate the system stability through eigenvalue analysis. The sensitivity to the control parameters is also presented to identify the validity of the controller design. The analysis results prove that the proposed controller provides stable and reliable operation, with the aim of maintaining the system voltage and frequency within acceptable limits.

II. Small-Signal Model of Autonomous Microgrid

In this paper, the small-signal dynamic model of the microgrid is divided into three individual sub-models, namely: inverter, network, and load. The model of the inverter includes the dynamics of the power controller, current controller, an output LC filter and the coupling inductance (if applicable). These dynamics are described based on their own reference $d-q$ frame, while for the purpose of the whole microgrid analysis, all the sub-models must be represented in a common reference $D-Q$ frame, so the inverter output signals can be converted into a common reference $D-Q$ frame using the following transformation technique [7]:

$$[f_{DQ}] = [T][f_{dq}] \tag{1}$$

$$[T] = \begin{bmatrix} cos(\theta) & -sin(\theta) \\ sin(\theta) & cos(\theta) \end{bmatrix} \tag{2}$$

where $\theta = \omega_s t + \theta_o$ is the synchronous rotating angle, θ_o represents the initial value.

A. State-Space Model of a 3-phase VSI System

The schematic diagram of the controlled VSI system is shown in Fig. 2. This system can be divided into two main circuits. First, the power circuit that includes the inverter and the output LC filter. Second, the control circuit which involves the power controller, current controller, and the power calculation loop that sets the feedback voltage and frequency values. Assuming that the DG unit is a constant DC source, the dynamic of the DC bus can be ignored. Also, because the inverter is a switch-mode device with the switching frequency sufficiently high, thus the switching action does not impact the states when a good attenuation of the switching frequency ripple is achieved through the output LC filter [8]. In this work, the state-space model of the remaining parts are developed as follows:

1) Power Controller: Fig. 3 shows the block diagram of the proposed power controller. System voltage and frequency are regulated with standard PI controllers based on real-time self-tuning method using the PSO algorithm. This controller represents the outer control loop which is employed to generate the reference current vectors i_d^* and i_q^*, so a relatively slow change of the reference current trajectory would ensure high quality of the inverter output power, which indicates that the control objective has been achieved. The corresponding state-space equations can be expressed as:

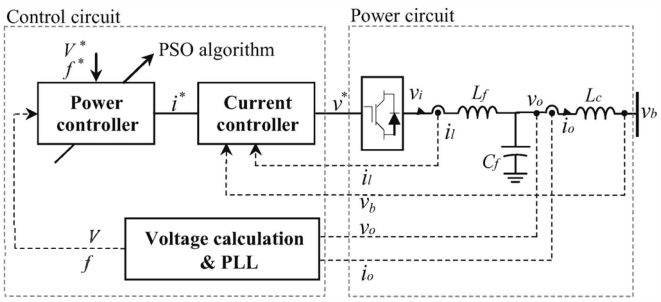

Fig. 2. The controlled VSI system

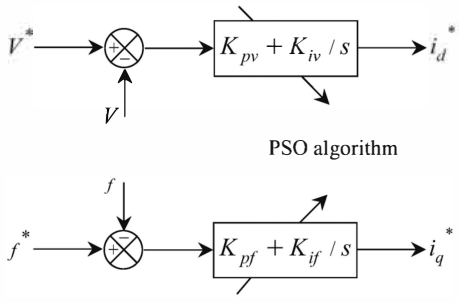

Fig. 3. The block diagram of the proposed power controller

$$\frac{d\gamma_d}{dt} = V^* - V, \qquad \frac{d\gamma_q}{dt} = f^* - f \tag{3}$$

and the output equations are given by:

$$i_d^* = K_{pv}(V^* - V) + K_{iv}\gamma_d \tag{4}$$

$$i_q^* = K_{pf}(f^* - f) + K_{if}\gamma_q \tag{5}$$

Since the input to the power controller can be divided into two terms: the reference and the feedback inputs, the linearized small-signal state-space equations can be written as:

$$\dot{[\triangle\gamma_{dq}]} = A_p\left[\triangle\gamma_{dq}\right] + B_{p_1}\left[\triangle V^* \ \triangle f^*\right]^T + B_{p_2}\left[\triangle V \ \triangle f\right]^T \tag{6}$$

where

$\triangle\gamma_{dq} = \begin{bmatrix} \triangle\gamma_d & \triangle\gamma_q \end{bmatrix}^T$, $A_p = [0]$, $B_{p_1} = \begin{bmatrix} 1 & 0 \\ 0 & 1 \end{bmatrix}$

$B_{p_2} = \begin{bmatrix} -1 & 0 \\ 0 & -1 \end{bmatrix}$

$$\left[\triangle i_{dq}^*\right] = C_p\left[\triangle\gamma_{dq}\right] + D_{p_1}\left[\triangle V^* \ \triangle f^*\right]^T + D_{p_2}\left[\triangle V \ \triangle f\right]^T \tag{7}$$

where

$\triangle i_{dq}^* = \begin{bmatrix} \triangle i_d^* & \triangle i_q^* \end{bmatrix}^T$, $C_p = \begin{bmatrix} K_{iv} & 0 \\ 0 & K_{if} \end{bmatrix}$

$D_{p_1} = \begin{bmatrix} K_{pv} & 0 \\ 0 & K_{pf} \end{bmatrix}$, $D_{p_2} = \begin{bmatrix} -K_{pv} & 0 \\ 0 & -K_{pf} \end{bmatrix}$

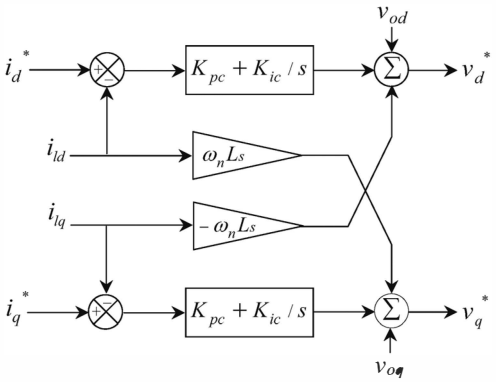

Fig. 4. The block diagram of the current controller

2) Current Controller: Fig. 4 shows the block diagram of the current controller, the objective of this controller is to ensure accurate tracking and short transients of the inverter output current. This controller is usually used in such a way that the voltage is applied to the inductive $R-L$ impedance, so that an impulse current in the inductor has a minimum error. Two PI regulators are used to eliminate current error, and both the inverter current loop and the grid voltage feed-forward loop are employed to improve the steady-state and dynamic performance. Here, the coupling inductance is not considered $(v_b = v_o)$, so the corresponding state-space equations can be expressed as:

$$\frac{d\phi_d}{dt} = i_d^* - i_{ld}, \qquad \frac{d\phi_q}{dt} = i_q^* - i_{lq} \tag{8}$$

and the output equations are given by:

$$v_d^* = v_{od} - \omega_n L_s i_{lq} + K_{pc}(i_d^* - i_{ld}) + K_{ic}\phi_d \tag{9}$$

$$v_q^* = v_{oq} + \omega_n L_s i_{ld} + K_{pc}(i_q^* - i_{lq}) + K_{ic}\phi_q \tag{10}$$

The linearized small-signal state-space equations can be written as:

$$\dot{[\triangle\phi_{dq}]} = A_c\left[\triangle\phi_{dq}\right] + B_{c_1}\left[\triangle i_{dq}^*\right] + B_{c_2}\begin{bmatrix}\triangle i_{ldq}\\ \triangle v_{odq}\\ \triangle i_{odq}\end{bmatrix} \tag{11}$$

where

$\triangle\phi_{dq} = \begin{bmatrix}\triangle\phi_d & \triangle\phi_q\end{bmatrix}^T$, $A_c = [0]$, $B_{c_1} = \begin{bmatrix}1 & 0\\ 0 & 1\end{bmatrix}$

$B_{c_2} = \begin{bmatrix}-1 & 0 & 0 & 0 & 0 & 0\\ 0 & -1 & 0 & 0 & 0 & 0\end{bmatrix}$

$$\left[\triangle v_{dq}^*\right] = C_c\left[\triangle\phi_{dq}\right] + D_{c_1}\left[\triangle i_{dq}^*\right] + D_{c_2}\begin{bmatrix}\triangle i_{ldq}\\ \triangle v_{odq}\\ \triangle i_{odq}\end{bmatrix} \tag{12}$$

$C_c = \begin{bmatrix}K_{ic} & 0\\ 0 & K_{ic}\end{bmatrix}$, $D_{c_1} = \begin{bmatrix}K_{pc} & 0\\ 0 & K_{pc}\end{bmatrix}$

$D_{c_2} = \begin{bmatrix}-K_{pc} & -\omega_n L_s & 1 & 0 & 0 & 0\\ \omega_n L_s & -K_{pc} & 0 & 1 & 0 & 0\end{bmatrix}$

3) Output LC Filter and Coupling Inductance : Assuming that the inverter drives perfect tracking $(v_i = v^*)$, and for further investigation of using the coupling inductance, the small-signal state-space equations of the output LC filter and the coupling inductance can be expressed as:

$$\frac{di_{ld}}{dt} = -\frac{R_f}{L_f}i_{ld} + \omega i_{lq} + \frac{1}{L_f}v_{id} - \frac{1}{L_f}v_{od} \tag{13}$$

$$\frac{di_{lq}}{dt} = -\frac{R_f}{L_f}i_{lq} - \omega i_{ld} + \frac{1}{L_f}v_{iq} - \frac{1}{L_f}v_{oq} \tag{14}$$

$$\frac{dv_{od}}{dt} = \omega v_{oq} + \frac{1}{C_f}i_{ld} - \frac{1}{C_f}i_{od} \tag{15}$$

$$\frac{dv_{oq}}{dt} = -\omega v_{od} + \frac{1}{C_f}i_{lq} - \frac{1}{C_f}i_{oq} \tag{16}$$

$$\frac{di_{od}}{dt} = -\frac{R_c}{L_c}i_{od} + \omega i_{oq} + \frac{1}{L_c}v_{od} - \frac{1}{L_c}v_{bd} \tag{17}$$

$$\frac{di_{oq}}{dt} = -\frac{R_c}{L_c}i_{oq} - \omega i_{od} + \frac{1}{L_c}v_{oq} - \frac{1}{L_c}v_{bq} \tag{18}$$

The linearized small-signal state-space equations can be written as:

$$\dot{\begin{bmatrix}\triangle i_{ldq}\\ \triangle v_{odq}\\ \triangle i_{odq}\end{bmatrix}} = A_{LCL}\begin{bmatrix}\triangle i_{ldq}\\ \triangle v_{odq}\\ \triangle i_{odq}\end{bmatrix} + B_{LCL1}\left[\triangle v_{idq}\right] + B_{LCL2}\left[\triangle v_{bdq}\right] \tag{19}$$

where

$$A_{LCL} = \begin{bmatrix}\frac{-R_f}{L_f} & \omega & \frac{-1}{L_f} & 0 & 0 & 0\\ -\omega & \frac{-R_f}{L_f} & 0 & \frac{-1}{L_f} & 0 & 0\\ \frac{1}{C_f} & 0 & 0 & \omega & \frac{-1}{C_f} & 0\\ 0 & \frac{1}{C_f} & -\omega & 0 & 0 & \frac{-1}{C_f}\\ 0 & 0 & \frac{1}{L_c} & 0 & \frac{-R_c}{L_c} & \omega\\ 0 & 0 & 0 & \frac{1}{L_c} & -\omega & \frac{-R_c}{L_c}\end{bmatrix}$$

$$B_{LCL1} = \begin{bmatrix}\frac{1}{L_f} & 0\\ 0 & \frac{1}{L_f}\\ 0 & 0\\ 0 & 0\\ 0 & 0\\ 0 & 0\end{bmatrix}, B_{LCL2} = \begin{bmatrix}0 & 0\\ 0 & 0\\ 0 & 0\\ 0 & 0\\ \frac{-1}{L_c} & 0\\ 0 & \frac{-1}{L_c}\end{bmatrix}$$

For the reason that the inverter is modeled based on its own reference $d-q$ frame, the inverter output current $\triangle i_{odq}$ must be expressed in a common reference $D-Q$ frame using the transformation technique given by (1) as follows:

$$\left[\triangle i_{oDQ}\right] = [T]\left[\triangle i_{odq}\right] \tag{20}$$

In contrast, the bus voltage (v_{bdq}) is the input signal to the inverter model which is represented in a common reference $D-Q$ frame, so the bus voltage can be converted into the inverter reference $d-q$ frame using the inverse transformation technique as follows:

$$\left[\triangle v_{bdq}\right] = [T]^{-1}\left[\triangle v_{bDQ}\right] \tag{21}$$

The overall state-space model of the inverter can be defined by combining the state-space equations of the power controller, current controller, and the output LC filter given by (6), (7), (11), (12), (19), (20) and (21), respectively. The dynamic model of the inverter can be expressed as:

$$\dot{[\triangle x_{inv}]} = A_{inv_1}[\triangle x_{inv}] + A_{inv_2}[\triangle V^* \triangle f^*]^T + A_{inv_3}[\triangle V \triangle f]^T + B_{inv}[\triangle v_{bDQ}] \quad (22)$$

$$[\triangle i_{oDQ}] = C_{inv}[\triangle x_{inv}] \quad (23)$$

where

$$[\triangle x_{inv}] = \begin{bmatrix} \triangle\gamma_{dq} & \triangle\phi_{dq} & \triangle i_{ldq} & \triangle v_{odq} & \triangle i_{odq} \end{bmatrix}^T$$

$$A_{inv_1} = \begin{bmatrix} B_{c_1}C_p & 0 & B_{c_2} \\ B_{LCL_1}D_{c_1}C_p & B_{LCL_1}C_c & A_{LCL} \\ & & +B_{LCL_1}D_{c_2} \\ & & +B_{LCL_2}T^{-1} \end{bmatrix}_{10\times 10}$$

$$A_{inv_2} = [B_{p_1} + (B_{c_1}D_{p_1}) + (B_{LCL_1}D_{c_1}D_{p_1})]_{2\times 2}$$
$$A_{inv_3} = [B_{p_2} + (B_{c_1}D_{p_2}) + (B_{LCL_1}D_{c_1}D_{p_2})]_{2\times 2}$$
$$B_{inv} = B_{LCL_2}[T]^{-1} \qquad C_{inv} = \begin{bmatrix} 0 & 0 & \dots & T \end{bmatrix}_{2\times 10}$$

B. State-Space Model of the Network and Load

The small-signal state-space model of the network and load are reported in [5]. Assuming that there are number of loads (L) and number of network nodes (N), thus LN is the number of lines, the corresponding state-space equation of the load can be written as:

$$\dot{[\triangle i_{loadDQ}]} = A_{load}[\triangle i_{loadDQ}] + B_{load}[\triangle v_{bDQ}] \quad (24)$$

In (24), for the i^{th} load connected to the j^{th} node:

$$[\triangle i_{loadDQ}] = [\triangle i_{loadDQ1}\ \triangle i_{loadDQ2} \dots \triangle i_{loadDQL}]^T$$

$$A_{loadi} = \begin{bmatrix} \frac{-R_{loadi}}{L_{loadi}} & \omega \\ -\omega & \frac{-R_{loadi}}{L_{loadi}} \end{bmatrix}$$

$$B_{loadi} = \begin{bmatrix} \frac{1}{L_{loadi}} & 0 \\ 0 & \frac{1}{L_{loadi}} \end{bmatrix}$$

Similarly, the state-space equation of the network can be expressed as:

$$\dot{[\triangle i_{lineDQ}]} = A_{net}[\triangle i_{lineDQ}] + B_{net}[\triangle v_{bDQ}] \quad (25)$$

In (25), for the network with i^{th} lines:

$$[\triangle i_{netDQ}] = [\triangle i_{netDQ1}\ \triangle i_{netDQ2} \dots \triangle i_{netDQLN}]^T$$

$$A_{neti} = \begin{bmatrix} \frac{-R_{linei}}{L_{linei}} & \omega \\ -\omega & \frac{-R_{linei}}{L_{linei}} \end{bmatrix}, i{=}1,2\dots LN$$

$$B_{neti} = \begin{bmatrix} \dots & \frac{1}{L_{linei}} & 0 & \dots & \frac{-1}{L_{linei}} & 0 & \dots \\ \dots & 0 & \frac{1}{L_{linei}} & \dots & 0 & \frac{-1}{L_{linei}} & \dots \end{bmatrix}$$

C. Overall Microgrid Model

The complete models of the inverter, network, and load can be combined to represent the microgrid model. The linearized equations given by (22), (24), and (25) show that the node voltage is the input to each model. To ensure well defined node voltage, a virtual resistance of a large magnitude ($rN \geqslant 1000\Omega$) is assumed between each network node and the ground [7]. The node voltage in terms of the inverter output current, load current, and the line current can be expressed as:

$$\triangle v_{bDQi} = rN(\triangle i_{oDQi} - \triangle i_{loadDQi} + \triangle i_{netDQi}) \quad (26)$$

The node voltage of the microgrid model is given by:

$$[\triangle v_{bDQi}] = R_N(M_{inv}[\triangle i_{oDQi}] + M_{load}[\triangle i_{loadDQi}] + M_{net}[\triangle i_{netDQi}]) \quad (27)$$

where R_N is the diagonal matrix of size $(2N \times 2N)$ with elements equal to rN. Assuming that I is the inverter, M_{inv} is a $(2N \times 2I)$ matrix that defines the inverter connection. For instance, if the I^{th} inverter is connected to the N^{th} node, the element $M_{inv(N,I)}$ is 1, and the rest of the elements of that row are 0. M_{load} is a $(2N \times 2L)$ matrix with -1 for the loads connected. Similarly M_{net} is a $(2N \times 2LN)$ matrix with ±1 elements taking into account the direction of the node current.

Using the linearized state-space equations (22), (24), and (25), the overall small-signal state-space model of the microgrid can be written as:

$$\dot{\begin{bmatrix} \triangle x_{inv} \\ \triangle i_{lineDQ} \\ \triangle i_{loadDQ} \end{bmatrix}} = A_{MG} \begin{bmatrix} \triangle x_{inv} \\ \triangle i_{lineDQ} \\ \triangle i_{loadDQ} \end{bmatrix} \quad (28)$$

where A_{MG} is the system state matrix which is given by (29). The stability analysis can be investigated through the eigen matrix A_{MG}

$$A_M = \begin{bmatrix} +B_{inv}R_N M_{inv}C_{inv} & B_{inv}R_N M_{net}\dots \\ B_{net}R_N M_{inv}C_{inv} & A_{net} + B_{net}R_N M_{net}\dots \\ B_{load}R_N M_{inv}C_{inv} & B_{load}R_N M_{net}\dots \\ & \dots B_{inv}R_N M_{load} \\ & \dots B_{net}R_N M_{load} \\ & \dots A_{load} + B_{load}R_N M_{load} \end{bmatrix} \quad (29)$$

D. Eigenvalue and Sensitivity Analysis

The eigenvalue analysis is the solution of the characteristic equation of the system state matrix. This solution produces eigenvalues (modes) that clarify the system stability around an operating point [3]. In conventional power systems, the eigenvalue analysis is extensively used to investigate the stability by identifying the oscillatory modes of the system components.

The sensitivity analysis is the method that measures the participation between state variables and the modes. The matrix of the participation factors can be defined once the eigenvalues are obtained. Using the right and left eigenvectors, the participation factors can be calculated as follows [9]:

TABLE II
EIGENVALUES AND THE PSO ALGORITHM RESULTS

Eigen values	Islanding mode				Load change			
	Real	Imaginary	PSO algorithm results		Real	Imaginary	PSO algorithm results	
			Parameter	Value			Parameter	Value
1,2	-899.5546087	±328.7569687	K_{pf}	3.010859051739	-899.4335534	±328.7635152	K_{pf}	2.561841587350
3,4	-40.29167979	±314.0002674	K_{if}	3.77937167e-04	-32.67425223	±314.0000938	K_{if}	3.77826970e-04
5,6	-227.8599673	±304.2016626	K_{pv}	-0.993692883859	-231.9889082	±305.5816123	K_{pv}	-1.012858708331
7,8	-189.6937473	±319.0404344	K_{iv}	0.003377691047	-184.0032894	±317.6541118	K_{iv}	0.003196350678
9,10	-45.51999665	±308.7666893			-45.51999665	±308.7666893		
11,12	-3.34904e-06	±2.27168e-05			-3.34904e-06	±2.27168e-05		
13,14	0	0			0	0		
15,16	-41.86424517	0			-42.69199105	0		
17,18	-129.0789640	0			-109.6873983	0		

TABLE I
NOMINAL SYSTEM PARAMETERS

Parameter	Value	Parameter	Value
DG unit	50 kW	$C_{dc-input}$	5000 µF
Frequency	50 Hz	Line resistance	0.4 Ω
R_f	1 Ω	Line inductance	2 mH
L_f	3 mH	K_{pc}	12.656
C_f	1500 µF	K_{ic}	0.00215

$$p_{ki} = l_k^i r_k^i \tag{30}$$

where p_{ki} is the participation of the i^{th} mode in the k^{th} state, l_k^i and r_k^i are the left and right eigenvectors, respectively.

E. PSO Algorithm

The PSO algorithm is an evolutionary computation technique proposed by Kennedy and Eberhart in 1995. The basic concept of this technique is to simulate the social behavior of the swarm in nature such as schools of fish or flocks of birds [10]. To solve the optimization problem, this algorithm evaluates itself based on the movement of each particle as well as the swarm collaboration [11].

The PSO search process mainly depends on each particle's position and velocity update in the specific dimension using the following equations [12]:

$$V_i^{k+1} = w.V_i^k + c_1.r_1\left[X_{pbest}^k - X_i^k\right] + c_2.r_2\left[X_{gbest}^k - X_i^k\right] \tag{31}$$

$$X_i^{k+1} = X_i^k + V_i^{k+1} \tag{32}$$

where i is the index of the particle; V_i^k, X_i^k are the velocity and position of particle *i* at iteration *k,* respectively; w is the inertia constant; c_1 and c_2 are the cognitive coefficients; r_1 and r_2 are random values which are generated for each velocity update; X_{gbest} and X_{pbest} are the global and local best positions, respectively.

To evaluate the search process, the *Integral Time Absolute Error* ($ITAE$) given by (33) is considered as an objective (fitness) function which calculates Simpson's 1/3 rule. The process can be terminated either when the algorithm completes the maximum number of iterations, or else when it achieves an acceptable fitness value.

$$ITAE = \int_0^\infty t|e(t)|dt \tag{33}$$

TABLE III
PARTICIPATION FACTORS OF THE SYSTEM STATES

States	Eigenvalues (islanding mode)								
	1,2	3,4	5,6	7,8	9,10	11,12	13,14	15,16	17,18
γ_{dq}							1		
ϕ_{dq}						0.5			
i_{ldq}					0.5				
v_{odq}	0.3								
i_{odq}	0.73		0.46	0.23					
V^*, f^*								1	
V, f									1
i_{line}	0.06	0.1							
i_{load}		0.4	0.27	0.35					

III. MODELING RESULTS

The model depicted in Fig. 2 is simulated using MATLAB/Simulink environment with the parameters given in Table I that represent the nominal operating condition. In this paper, the small-signal dynamic model is developed as in (28). Using the eigenvalue analysis, the stability has been investigated through the location of the eigenvalues of the system state matrix A_{MG} in the complex plane.

Table II shows the results of the eigenvalue analysis of the oscillatory modes and the PSO algorithm. This analysis demonstrates that the model exhibits 9 eigen pairs: 6 complex conjugates and 3 real parts. The eigenvalues 1-14 represent the seven oscillatory modes of the controlled VSI system, all these modes are negative except 13 and 14 which are zero. That indicates the system has good dynamic properties under the given operating condition and the power control parameters which are found by the PSO algorithm. The negative real pairs (15,16) and (17,18) describe the oscillatory modes of the network line and load, respectively. In the simulation results, the load is considered to be active power for simplicity and set to 4.65 p.u. for the islanding mode, then reduced to 4.55 p.u. to emulate the load change condition. Figs. 5 and 6 show that the power controller provides an excellent response of regulating the microgrid voltage and frequency. Thus, the eigenvalue analysis and the simulation results confirm that the proposed controller provides stable and reliable operation based on the PSO algorithm.

Table III presents the model's participation factors which are used for measuring the influence of the states in the modes, the states who heavily impact the modes have the maximum value in each row. In this paper, this analysis is only described

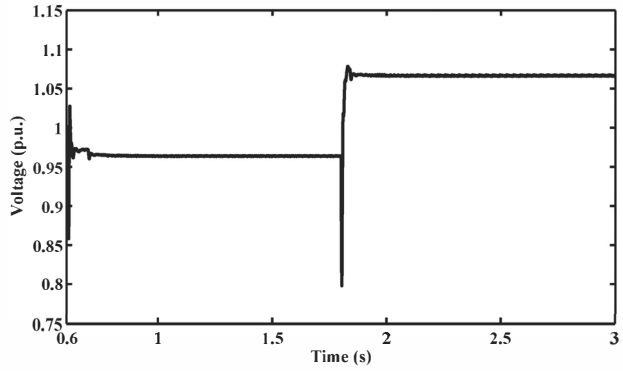

Fig. 5. The system voltage regulated by the proposed controller

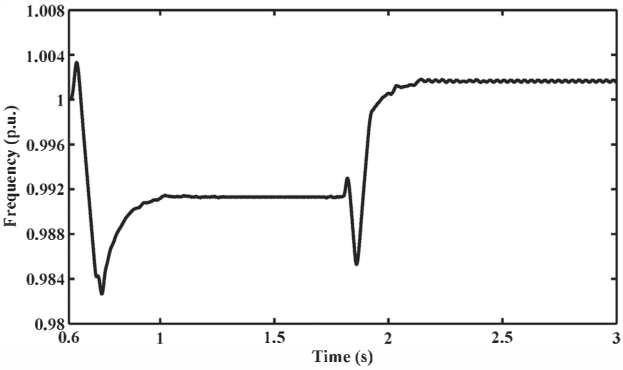

Fig. 6. The system frequency regulated by the proposed controller

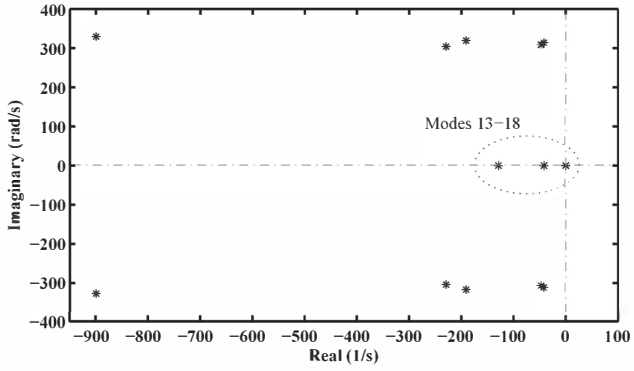

Fig. 7. Eigenvalues of the islanding mode

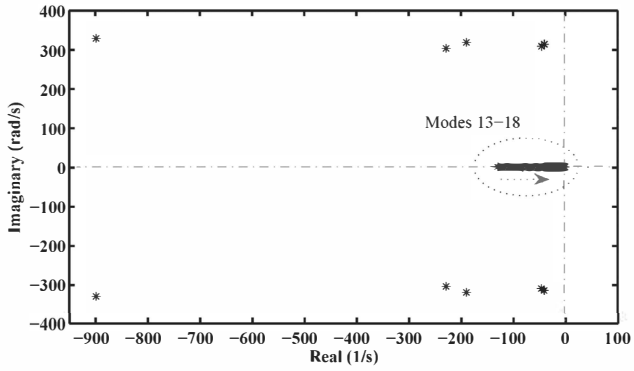

Fig. 8. Eigenvalue locus of changing K_{pv} and K_{pf}

for the islanding mode in order to explain the sensitivity of the proposed power controller. While the factors less than 0.1 are ignored, the states of the power controller participate with the maximum values in modes 13-18. To confirm that these modes are largely sensitive to the state variables of the power controller, Figs. 7 and 8 show that changing K_{pf} and K_{pv} moves these modes to the right hand side, thus the system becomes more oscillatory and unstable.

IV. Conclusion

In this paper, the small-signal state-space model has been developed for an inverter based DG unit in an autonomous microgrid operation. This model is used to examine the system stability by using the eigenvalue analysis in order to evaluate the system operation around the given operating point and under the proposed power controller. The system dynamic model is constructed based on the three main sub-models, namely: inverter, network, and load. The eigenvalue analysis is driven by the linearized system state matrix to investigate the system oscillatory mode and the sensitivity to controller parameters. This controller is proposed to improve the quality of the power supply by regulating the voltage and frequency when the microgrid is in islanding mode or during load change. Also, the PSO algorithm has been incorporated to find the optimal control parameters. The eigenvalue analysis and the simulation results confirm that the system produces stable and reliable operation under the proposed power controller.

References

[1] R. H. Lasseter, "Microgrids,"
Meeting, 2002. IEEE, vol. 1, pp. 305–308 vol.1.

[2] R.Strzelecki and G.Benysek, *Power electronics in smart electrical energy networks*. Verlag London: Springer, 2008.

[3] L. L. Grigsby, *Power system stability and control*. Boca Raton: CRC Press, 2007, 2007006226 editor, Leonard Lee Grigsby. ill. ; 27 cm. Includes bibliographical references and index.

[4] Z. Yu, J. Zhenhua, and Y. Xunwei, "Small-signal modeling and analysis of parallel-connected voltage source inverters,"
Motion Control Conference, 2009. IPEMC '09. IEEE 6th International, pp. 377–383.

[5] N. Pogaku, M. Prodanovic, and T. C. Green, "Modeling, analysis and testing of autonomous operation of an inverter-based microgrid,"
Electronics, IEEE Transactions on, vol. 22, no. 2, pp. 613–625, 2007.

[6] F. Katiraei and M. R. Iravani, "Power management strategies for a microgrid with multiple distributed generation units,"
IEEE Transactions on, vol. 21, no. 4, pp. 1821–1831, 2006.

[7] R. Majumder, B. Chaudhuri, A. Ghosh, G. Ledwich, and F. Zare, "Improvement of stability and load sharing in an autonomous microgrid using supplementary droop control loop,"
Transactions on, vol. 25, no. 2, pp. 796–808, 2010.

[8] N. Kroutikova, C. A. Hernandez-Aramburo, and T. C. Green, "State-space model of grid-connected inverters under current control mode,"
Electric Power Applications, IET, vol. 1, no. 3, pp. 329–338, 2007.

[9] S. Li, E. H. Abed, M. A. Hassouneh, Y. Huizhong, and M. S. Saad, "Mode in output participation factors for linear systems,"
Control Conference (ACC), 2010, pp. 956–961.

[10] J. Kennedy and R. Eberhart, "Particle swarm optimization,"
Networks, 1995. Proceedings., IEEE International Conference on, vol. 4, pp. 1942–1948 vol.4.

[11] Yang and Xin-She, *Engineering optimization: An introduction with metaheuristic application*. Hoboken: John Wiley, 2010.

[12] Y. del Valle, G. K. Venayagamoorthy, S. Mohagheghi, J. C. Hernandez, and R. G. Harley, "Particle swarm optimization: Basic concepts, variants and applications in power systems,"
Transactions on, vol. 12, no. 2, pp. 171–195, 2008.